Research Article | Vol. 30, No. 13 / 20 Jun 2022 / Optics Express 22364

Optics EXPRESS

2m-distance external cavity VECSEL for wireless charging applications

ZHUO ZHANG,[1,2] JIANWEI ZHANG,[1,*] YINLI ZHOU,[1] XING ZHANG,[1] ZHIWEI LI,[1,2] JIYE ZHANG,[1] JUN ZHANG,[1] YUXIANG GONG,[1,2] TIANJIAO LIU,[1,2] JINGFEI MU,[1,2] YONGQIANG NING,[1] LI QIN,[1] AND LIJUN WANG[1]

[1] *State Key Laboratory of Luminescence and Applications, Changchun Institute of Optics, Fine Mechanics and Physics, Chinese Academy of Sciences, Changchun, Jilin 130033, China*
[2] *University of Chinese Academy of Sciences, Beijing 100049, China*
[*] *zjw1985@ciomp.ac.cn*

Abstract: We characterize laser generation in an ultralong air cavity (several meters in length) using an optical-pumped semiconductor gain chip for laser wireless charging applications. The study realizes laser generation in an external air cavity with a length of 200 cm, for the first time, and achieves a maximum output laser power of more than 86.3 mW. Furthermore, the laser oscillation can be maintained even when the output mirror of laser is off-axis within 1.6 cm. Thus, a long external cavity laser would ease the alignment between the laser beam and charging terminal, making it suitable for laser wireless charging applications.

1. Introduction

Portable electronic devices such as mobile phones are becoming increasingly popular. Therefore, manufacturers are actively developing more convenient wireless charging technologies [1,2]. In recent years, electromagnetic induction or microwaves have been used for wireless charging [3–5]. However, both methods have limitations. For example, the charging distance for electromagnetic induction is only approximately 1 cm. By contrast, although microwaves have a long transmission distance, realizing a large charging distance requires high-energy microwave radiation poses health risks [6]. Owing to rapid developments in laser technology, light can now be used as the power carrier to achieve long-distance and high-efficiency wireless energy transmission [7]. A laser with good directivity and high power transmission density can achieve high-efficiency wireless energy transmission. In recent years, lasers have been widely applied in wireless charging technologies [8–10]. An oscillating external cavity affords unique advantages in laser wireless charging. For example, the output mirror of the external cavity can be directly integrated into the receiving end system as a receiving mirror. When intracavity laser oscillation is blocked by an external object, the laser generation process is interrupted, and the blocked object is not damaged [11]. Since optical signals can simultaneously transmit power and information, the wireless charging system could also function similarly [12–14]. Using a semiconductor laser gain medium affords advantages including high gain, low cost, and small volume [15,16]. Vertical external-cavity surface-emitting lasers (VECSELs) with high output power and high beam quality are an ideal light source for wireless applications [17,18].

VECSEL technology is relatively mature, and considerable progress has been made in realizing laser mode control and wavelength control [19,20]. Through intracavity frequency conversion, the luminescent wavelength from ultraviolet to long-wave infrared has been covered [21–24]. Various cavity structures have been proposed to improve the efficiency of gain chips, and the incident pump power to output power conversion efficiency has been improved to a maximum of 28% [25]. VECSELs with an external cavity can realize frequency modulation and pulse

#457112 https://doi.org/10.1364/OE.457112
Journal © 2022 Received 27 Feb 2022; revised 20 Apr 2022; accepted 17 May 2022; published 6 Jun 2022

Optics EXPRESS

generation [26,27]. Therefore, VECSELs with an ultralong external cavity can also be used in wireless communication technology. However, few studies have investigated the ultralong cavity oscillation and off-axis function of VECSELs with a semiconductor gain chip.

This study develops a method to achieve ultralong external cavity laser oscillation by optimizing the optical path structure of an optically pumped VECSEL. First, we introduce the design principle of ultralong cavity VECSEL. Second, we analyze the output power and off-axis characteristics of VECSELs with different cavity lengths. Finally, we analyze the wavelength, spectrum, and divergence angle of VECSELs with a cavity length of 200 cm.

2. System overview and simulation details

Figure 1 shows a schematic of the VECSEL structure for realizing long-cavity long-laser oscillation. We adopt the classical V-shaped oscillating cavity structure, where M_{out} and M_{back} are the laser output mirror and back mirror of the oscillating cavity, respectively; M_{back} is a plane mirror with high reflectivity (≥99.9%); M_{out} is a flat concave mirror with a reflectivity of approximately 97.5%, and Lens 1, Lens 2, and Lens 3 are intracavity beam conversion lenses. To reduce the loss of intracavity optical oscillation, the reflectivity of Lens 1, Lens 2, and Lens 3 is less than 0.1%. By suitably designing the optical parameters of Lens 1, Lens 2, Lens 3, M_{back}, gain chip, and M_{out}, a compact configuration scheme can be obtained, and a meter-level ultralong laser oscillation cavity between Lens 2 and Lens 3 can be guaranteed. We realize sufficient intracavity laser gain by using an external laser-pumped semiconductor gain chip to support intracavity laser oscillation [28]. Since the optical pumping structure has a high heat dissipation requirement for the gain chip, the gain chip is integrated on a thermoelectric cooler (TEC) to cool it rapidly, as shown in Fig. 1 [29]. The pump system consists of an 808 nm, fiber-coupled diode laser with a maximum output power of 100 W and a focusing lens group. The pump laser is focused on the gain chip at an incident angle of nearly 45°. The pump spot size and pump power density on the chip surface can be adjusted by the focusing lens group.

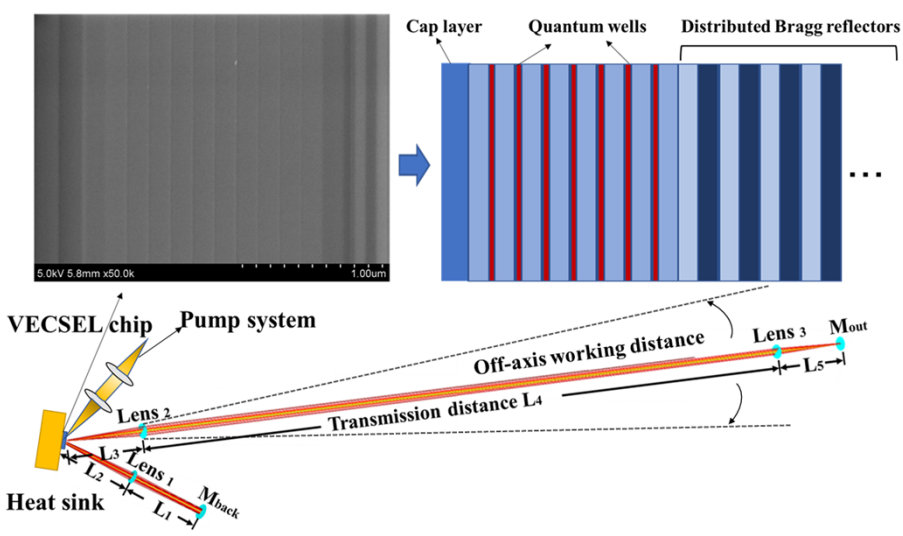

Fig. 1. Schematic of the working principle of a long-cavity VECSEL, SEM diagram of the gain chip internal luminescence area, and schematic of the active region structure.

The gain chip consists of active region and 35 pairs of distributed Bragg reflector (DBR), partially shown in the SEM diagram in Fig. 1. The active region contains eight periodic $In_{0.17}Ga_{0.83}As$ quantum wells (QWs) placed at antinodes of the standing wave pattern of the

Optics EXPRESS

optical field [30]. The layers between QWs contain the $GaAs_{0.92}P_{0.08}$ barriers and pump-absorbing GaAs layers. The tensile-strained $GaAs_{0.92}P_{0.08}$ layers serve as strain-compensating layers and are positioned on both sides of QWs. The 35 pairs of AlAs/GaAs DBR can provide high reflectivity of more than 99.9% near the lasing wavelength. The DBR serves as the laser beam steering mirror of the V-shaped oscillation cavity. The gain-chip structure is grown by MOCVD on the (100) GaAs substrate. To realize the GaAs substrate-removal by selective wet-chemical procedure, an GaInP etch-stop layer is also introduced between the substrate and gain-chip structure [31].

For the V-shaped resonator cavity shown in Fig. 1, the gain chip has a certain included angle with the external cavities on both sides; that is, DBR must provide a high reflectivity when light is not incident vertically. Figure 2 shows the reflection spectrum calculation results of DBR at different incident angles. The incident light is vertically incident from the air medium, and the reflection spectrum of the DBR mirror, which has nearly 100% reflectivity at nearly 50 nm on both sides of 980 nm, is shown in the blue solid line in Fig. 2. The DBR reflection spectrum with an incident light angle of 15 ° shifts by 10 nm to the short wave. As shown in the black dashed line in Fig. 2, it covers 920-1020 nm and can provide high reflectivity at 40 nm near the laser wavelength. The DBR reflection spectrum with an incident light angle of 30 ° drifts 40 nm to the short wave, as shown by the red dot dash line in Fig. 2, and can still cover the outgoing laser band. The included angle of the V-shaped cavity used in this study is about 24 °, and that between the cavities on both sides and gain chip is about 12 °. The DBR of gain chip can provide nearly 100% reflectivity near 980 nm at this incident angle.

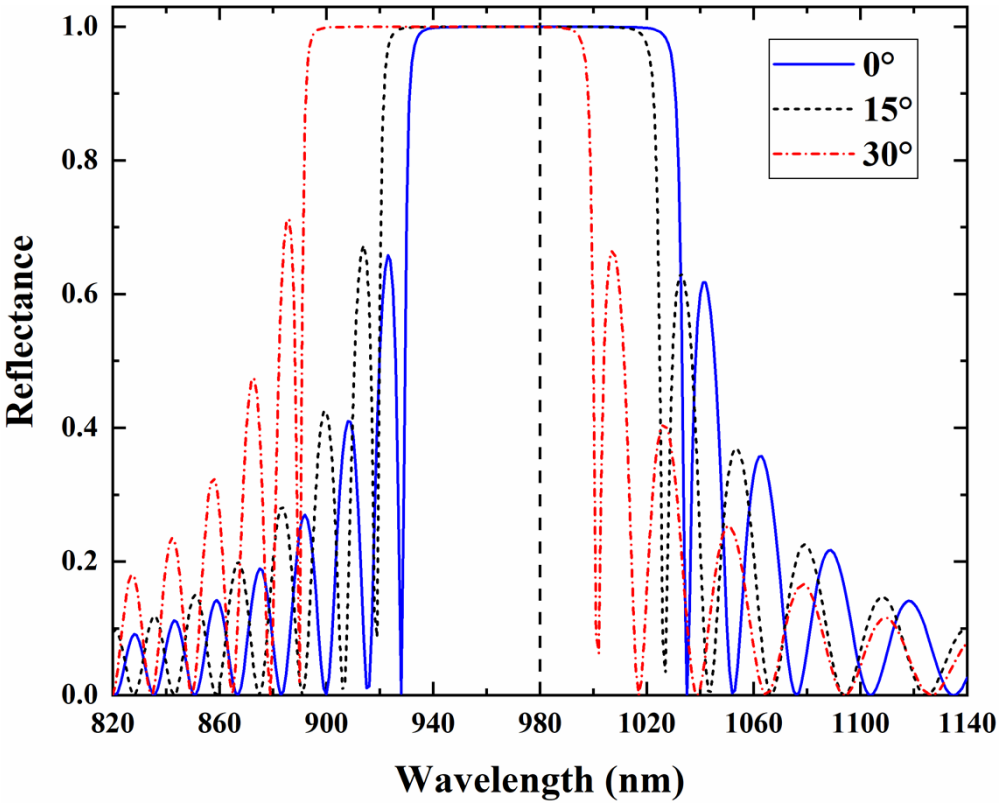

Fig. 2. The reflection spectrum of DBR to the incident light at different incident angles of 0 °, 15 ° and 30 °.

Optics EXPRESS

In the optical scheme shown in Fig. 1, the primary function of M_{back} and Lens 1 is to realize the compression and effective feedback of the gain chip spot, and the parameter and position design of Lens 2 and Lens 3 are essential for determining the length of the external cavity. In Fig. 1, the distance between Lens 2 and the gain chip is L_3, and the distance between Lens 2 and Lens 3 is L_4. In Fig. 3, we show the simulation results of the influence of L_3 and L_4 on the stability parameter of the external cavity laser oscillation when the focal lengths of Lens 1, Lens 2, and Lens 3 are all 15 cm. The laser cavity is designed based on the generalised ABCD matrix method [32]. Based on this method, the beam propagation in the long and stable cavity with complex mirrors can be gained and analyzed. The stable travelling of optical beam within the cavity thus can be gained when the light beam oscillates in the laser cavity many times without leakage [33]. For the stable oscillation cavity, the absolute value of stability parameter calculated from ABCD matrix should be between 0 to 1 [34]. Figure 3 depicts the stability parameter values of the laser cavity in different colors. The area where the laser cavity cannot work stably is marked in dark blue. Figure 3 shows that the smaller the L_3 value, the greater is the L_4 value to ensure the stability of the cavity. When L_3 decreases to approximately 160 mm, stable oscillation in the cavity can be achieved when L_4 is increased from 500 to 4000 mm. Therefore, selecting Lens 2 to ensure that the external cavity has enough oscillation cavity length and reduce the gain chip length L_3 is beneficial for realizing a compact wireless charging terminal.

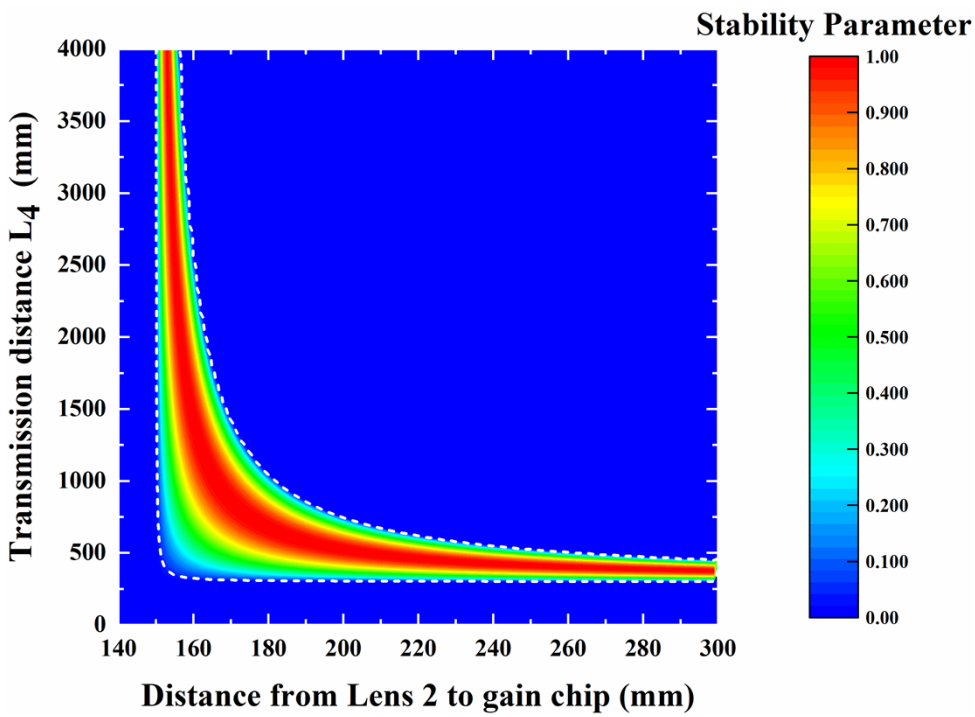

Fig. 3. Influence of cavity lengths L_4 and L_3 in the VECSEL on the stability parameter in the cavity. The area enclosed by the white dotted line is the working area for cavity stabilization.

For a wireless charging light source, L_4 in Fig. 1 is the working distance. In Fig. 3, when the distance between Lens 2 and the gain chip is approximately 150 mm, L_4 achieves stable intracavity laser oscillation at different lengths. Figure 4 shows the whole cavity internal spot transmission under this condition for L_4 values of 50, 100, and 200 cm. The fundamental mode spot size formula of Gaussian beam can simulate the change of spot size in laser cavity with

Optics EXPRESS

cavity length. To compare the spot distribution, we show the spot in the folded cavity in the form of straight transmission in Fig. 4. This figure shows the turning point of the light field, namely, the amplification of the spot distribution near the gain chip.

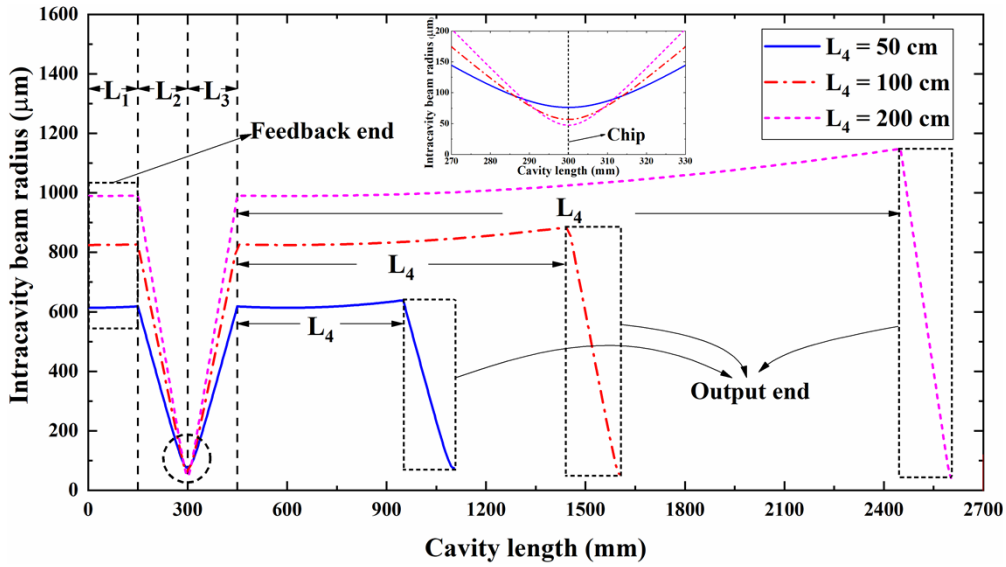

Fig. 4. VECSEL internal oscillating laser beam distribution for L_4 values of 50, 100, and 200 cm.

The spot size on the gain chip shows little change with the length of the external oscillation cavity. The length of the external cavity is 100 and 200 cm, and the corresponding spot radius is approximately 50 μm. Through the external cavity modulation of the long cavity, the laser mode corresponding to the small spot size is often a single mode [35,36].

In Fig. 4, the distance between the mirror group composed of M_{back} and Lens 1 and the gain chip is constant. The spot sizes on these two mirrors are almost the same because we choose a collimated lens. As the external cavity length increases from 50 to 100 cm, the spot radius of M_{back} and Lens 1 increases from 614 to 990 μm.

Similar to the feedback mirror group, the spot size of the output mirror group also increases with the change in the cavity length, and the spot size at Lens 3 in the output mirror group is slightly larger than that at M_{back} and Lens 1. At position Lens 3, as the external cavity length increases from 50 to 200 cm, the spot radius increases from 638 to 1145 μm. Since the Lens 3 has a focusing effect, the spot size is only 48 μm at the M_{out} position of the output mirror. This design ensures that only a small area of solar cells is needed to receive the entire laser light field; this is conducive to the integrated use of portable mobile terminals in the backend. Figure 4 shows that even if the external cavity length increases to 200 cm, the maximum spot radius at each optical lens position is just 1145 μm; this is beneficial to the miniaturization of the whole laser charging system.

3. Experimental results and discussion

As shown in Fig. 1, the gain chip provides optical gain for the system and determines the laser wavelength of the whole system owing to its DBR structure and the microcavity effect of the QW luminescence region [37]. The gain chip of our VECSEL is grown on GaAs (100) substrates cut into 3×3 mm^2 slices. We package the gain chip in an inverted form on a copper heat sink with TEC and remove its substrate so that the QW luminescence region is located on the surface.

Optics EXPRESS

Figure 5 shows test results of the photoluminescence (PL) spectrum and surface reflection spectrum of the gain chip at a TEC temperature of 0 °C. The PL peak of the gain chip, as shown in the figure, is at 972 nm. A prominent dent is seen at the center of the reflection band of the gain chip owing to the microcavity oscillation effect of the DBR and the luminescence region. The lowest point of the dent is at 977 nm; it determines the wavelength of the VECSEL. The gain peak closely matches the reflection spectrum at 0 °C.

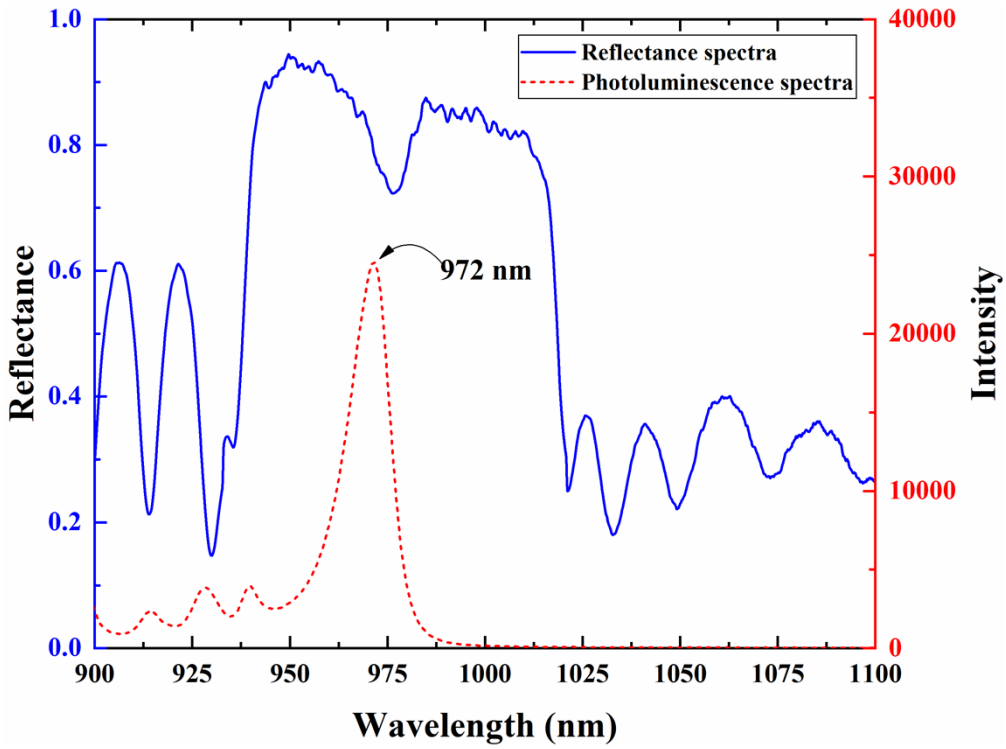

Fig. 5. 0 °C gain chip reflection spectrum (solid line) and PL spectrum from the InGaAs chip (red dash curve).

By using the scheme shown in Fig. 1, we successfully realized VECSEL operation under different external cavity lengths. Figure 6 shows the variation curves of the laser output power with the pump power for VECSELs with different external cavity lengths. As the pump power increases, the laser output power increases. Further, when the pump power increases to a certain value, owing to the restriction of the internal thermal effect, the laser output power exhibits an apparent rollover phenomenon. In Fig. 6, the excitation thresholds of VECSELs with different cavity lengths are very close because the change in cavity length does not affect the effective gain provided by the gain chip. The slope efficiencies of the power curves of VECSELs with different cavity lengths are significantly different. With an increase in the cavity length, the slope efficiency of the power curve exhibits a downward trend. The maximum output power of the VECSEL also decreases. When the cavity length increases from 50 to 200 cm, the maximum output power of the VECSEL decreases from 90.3 to 77.1 mW. After the gain chip is pumped by the pump light, the fluorescence produced by itself is not directional. The optical scheme in Fig. 1 indicates that the farther the optical mirror feedback system composed of Lens 3 and M_{out} is from the gain chip, the smaller is the proportion of fluorescence emitted by the gain chip that is fed back by the mirror group, i.e., the more is the amount of fluorescence that is lost. Therefore, the utilization efficiency of the whole pump light decreases with an increase in the

Optics EXPRESS

external cavity length; this explains why a VECSEL with a longer cavity length has lower slope efficiency. However, the pump light utilization efficiency decreases, indicating that the internal self-generated heat effect of the gain chip is severe. Therefore, with an increase in the external cavity length, the flip power of the VECSEL decreases.

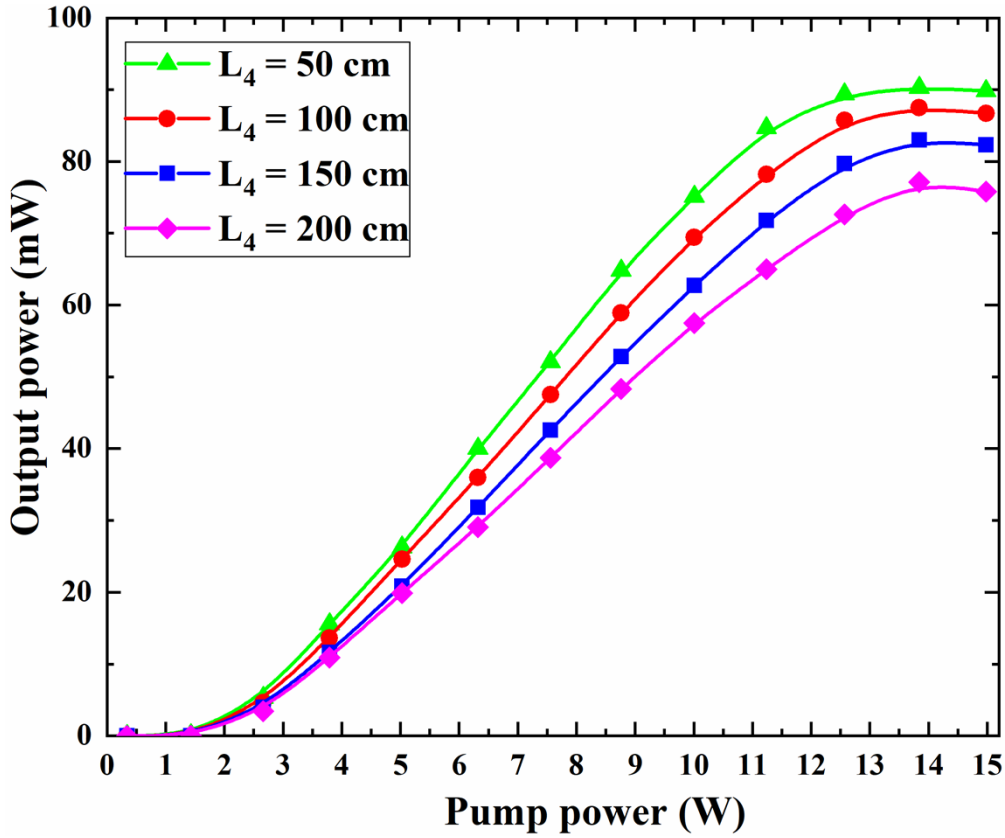

Fig. 6. VECSEL output power curves for different external cavity lengths at 0 °C.

To verify the above conjecture, we verify the off-axis operating characteristics of VECSELs with different cavity lengths. The off-axis distance refers to the offset distance between the central axis of output mirror group Lens 3 and M_{out} relative to the system axis (i.e., the central axis of Lens 2). When fully consistent with the central axis, we define the off-axis distance as 0. When the output mirror group is translated clockwise and anticlockwise relative to the central axis, we define the off-axis distance as negative and positive, respectively. The pump optical power is set at 11 W, and the output mirror group is placed at different off-axis distances and debugged to ensure the laser output. The variation curve of the laser power with the off-axis distance for VECSELs with different cavity lengths is obtained as shown in Fig. 7.

Figure 7 shows that when the central axis of the output mirror group Lens 3 and M_{out} matches the VECSEL system (Lens 2), the VECSEL has the maximum output power. In the region with a large off-axis distance, the power level of the VECSEL decreases with an increase in the off-axis distance. This is mainly because, in off-axis cases, the optical field intensity fed back to the gain chip by the output mirror group decreases, and the effective gain that can be obtained in the cavity also decreases.

Optics EXPRESS

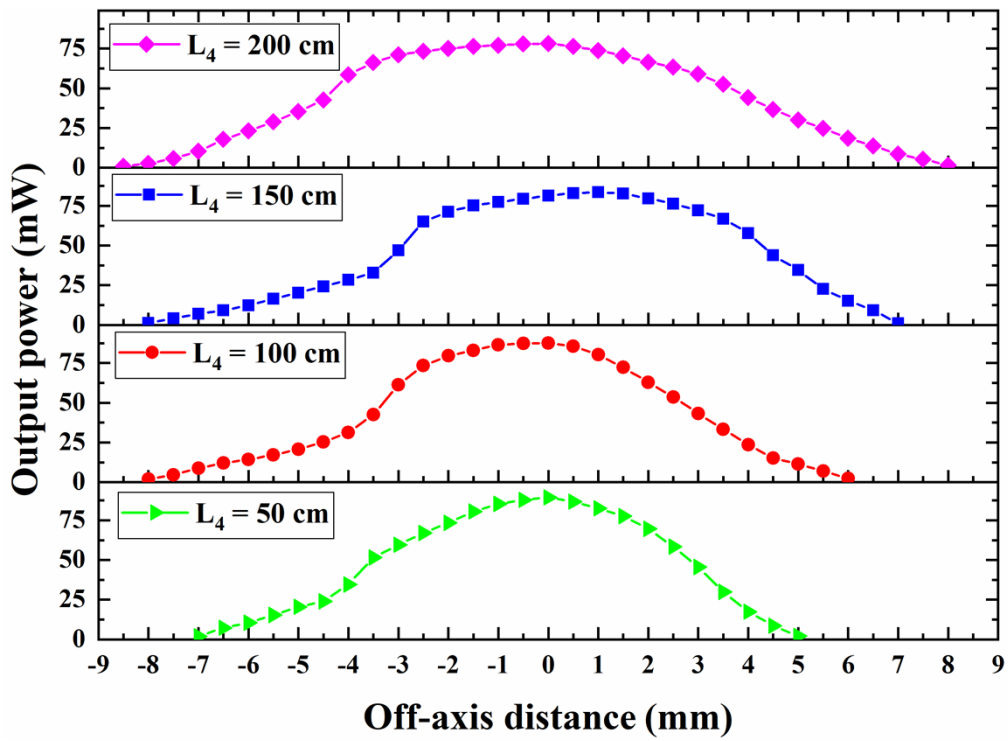

Fig. 7. VECSEL output power according to off-axis distance under different cavity lengths (L_4 = 50, 100, 150, and 200 cm). An off-axis distance of 0 indicates that the central axis of the output mirror group matches the central axis of the VECSEL system.

The simulation results in Fig. 4 indicate that the longer the cavity length, the larger is the spot at the output mirror position, and the larger is the off-axis distance. Therefore, in Fig. 6, with an increase in the external cavity length, the off-axis distance over which the VECSEL can operate increases gradually. When the external cavity length increases to 200 cm, the VECSEL still has more than 10% coaxial laser power at an off-axis distance of 7 mm. This shows that the VECSEL output can move freely over a distance of 14 mm. When the output mirror group is integrated

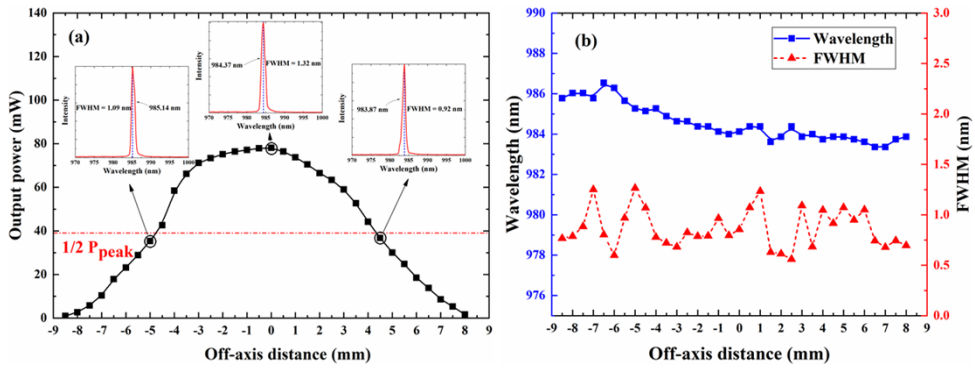

Fig. 8. (a). VECSEL typical laser spectra at different off-axis positions. (b) VECSEL laser wavelength and spectral half width at different off-axis distances with L_4 = 200 cm.

Optics EXPRESS

into the wireless charging terminal, a large free-moving distance is very beneficial to improve the alignment accuracy.

Figure 8(a) shows the typical laser spectrum of VECSEL at three off-axis positions when the external cavity length is 200 cm. Figure 8(b) shows the laser wavelength and spectral half-width of the VECSEL laser at different off-axis positions. The laser wavelength and spectral half-width of the laser oscillation at different off-axis distances change slightly. As the off-axis distance

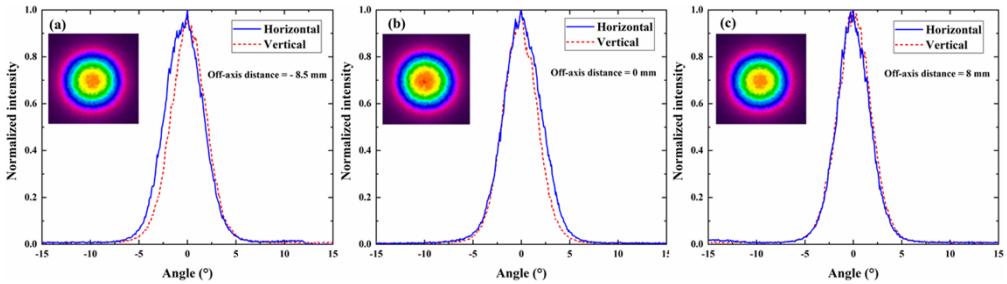

Fig. 9. Laser beam divergence angles with different off-axis distances: (a) -8.5, (b) 0, and (c) 8 mm. The inset shows the two-dimensional shape of the laser spot.

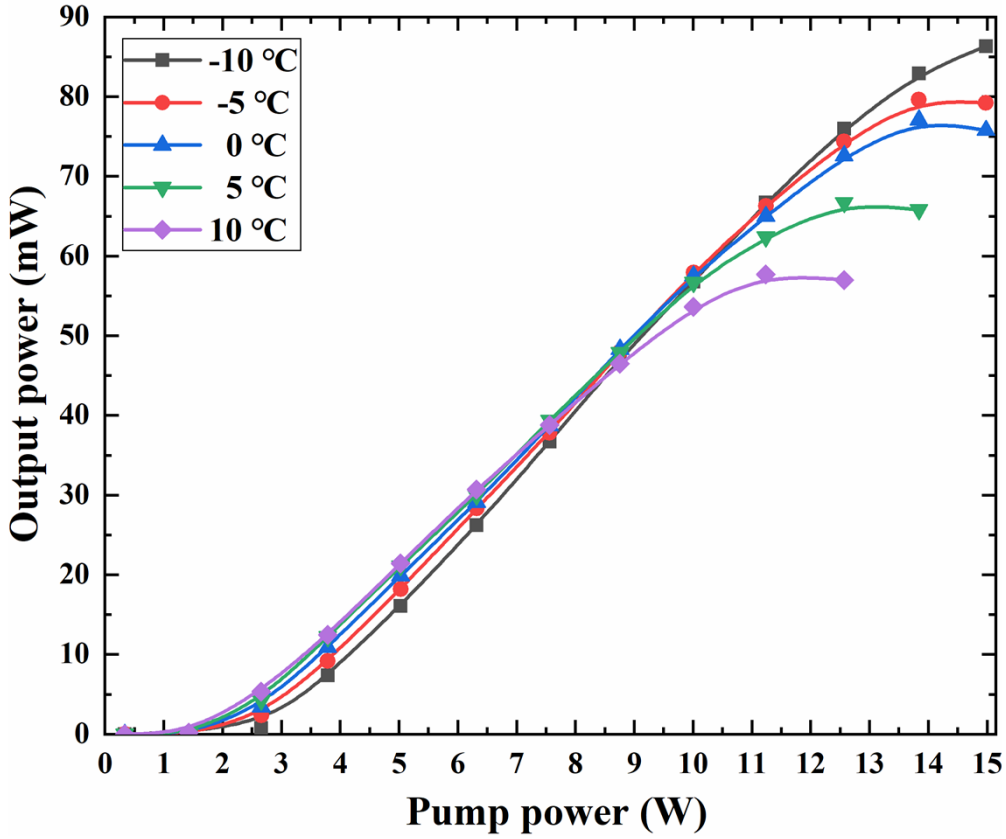

Fig. 10. VECSEL output power curve with an external cavity length of 200 cm at different operating temperatures.

Optics EXPRESS

changes from -8.5 to +8 mm, the laser wavelength fluctuates between 984 and 986 nm, and the corresponding laser spectral half-width fluctuates between 0.5 and 1.5 nm.

Figure 9 shows the test results of the laser divergence angle and spot morphology at different off-axis distances in Fig. 8(a). At three different off-axis positions, the laser divergence angles are 6.95°, 6.87°, and 6.75°, exhibiting circular symmetry. Further, the laser light field exhibits a Gaussian distribution.

Figure 10 shows the power curve of a long-cavity VECSEL at different base temperatures. With an increase in the base temperature, the internal temperature of the gain chip increases, and the heat dissipation rate decreases. Thus, the maximum output laser power of the VECSEL decreases considerably with an increase in the operating temperature. As shown in Fig. 5, there is a distance of about 5 nm between the peak of PL spectrum and cavity mode of the reflection spectrum. As the temperature rises, the PL spectrum shifts to longer wavelengths by ~ 0.3 nm K^{-1} [29]. The cavity mode of the reflection spectrum also shifts to longer wavelength with increasing temperature, but more slowly than the PL spectrum, typically at ~ 0.1 nm K^{-1} [29]. Therefore, due to the gain spectrum of the gain chip and detuning design of the laser cavity mode, the peak of PL spectrum is closer to the cavity mode with the increase of temperature, resulting in the decrease of the threshold power of the VECSEL [38].

4. Summary and outlook

In this study, we designed and fabricated an ultralong VECSEL resonator for laser wireless charging applications. By designing suitable optical element parameters in the cavity, it was proved theoretically that stable laser oscillation could be achieved in the external cavity over more than 400 cm, a typical indoor wireless laser charging distance. We realized stable intracavity oscillation with a cavity length of 200 cm and ensured a stable laser output when the output mirror group deviated from the central axis by 8 mm. The maximum laser power reached 86.3 mW; the laser beam exhibited a Gaussian spot morphology, and the beam divergence angle was only 6.87°. We believe that this study provides an effective solution for future wireless laser charging light sources. Taking advantage of the laser cavity characteristics, the existence of occlusion in the cavity will prevent the laser from outputting, which makes the proposed VECSEL scheme safer. The semiconductor gain material used in the proposed system has high gain and high efficiency and outputs a communication band laser through the gain band design. In future work, we will optimize the structure of the gain chip to further improve the laser power level and work efficiency and seek ways to increase the off-axis range. After optimizing the VECSEL system, different gain chips and modulation methods can be used to realize the synchronous transmission of wireless energy and information.

Funding. Key Projects of Jilin Province Science and Technology Development Plan, China (20200401006GX); National Natural Science Foundation of China (11774343, 61804087, 61874117); Major Program of the National Natural Science Foundation of China (62090060).

Disclosures. The authors declare no conflicts of interest.

Data availability. Data underlying the results presented in this paper are not publicly available at this time but may be obtained from the authors upon reasonable request.

References

1. L. Han and L. M. Li, "Integrated wireless communications and wireless power transfer: An overview," Physical Communication **25**(2), 555–563 (2017).
2. X. Lu, D. Niyato, P. Wang, D. I. Kim, and Z. Han, "Wireless charger networking for mobile devices: Fundamentals, standards, and applications," IEEE Wireless Commun. **22**(2), 126–135 (2015).
3. F. Shan, J. Z. Luo, W. W. Wu, and X. J. Shen, "Delay Minimization for Data Transmission in Wireless Power Transfer Systems," IEEE J. Select. Areas Commun. **37**(2), 298–312 (2019).
4. Q. Liu, J. Wu, P. Xia, S. Zhao, and L. Hanzo, "Charging Unplugged: Will Distributed Laser Charging for Mobile Wireless Power Transfer Work?" IEEE Trans. Veh. Technol. **11**(4), 36–45 (2016).

Optics EXPRESS

5. K. W. Choi, A. A. Aziz, D. Setiawan, N. M. Tran, L. Ginting, and D. I. Kim, "Distributed Wireless Power Transfer System for Internet of Things Devices," IEEE Internet Things J. **5**(4), 2657–2671 (2018).
6. N. Shinohara, "The wireless power transmission: inductive coupling, radio wave, and resonance coupling," Wiley Interdiscip. Rev. Energy Environ. **1**(3), 337–346 (2012).
7. J. P. Ding, W. W. Liu, I. Chih-Lin, H. Zhang, and H. Y. Mei, "Advanced Progress of Optical Wireless Technologies for Power Industry: An Overview," Appl. Sci. **10**(18), 6463 (2020).
8. J. Lim, T. S. Khwaja, and J. Ha, "Wireless optical power transfer system by spatial wavelength division and distributed laser cavity resonance," Opt. Express **27**(12), A924–A935 (2019).
9. P. Xu, W. Zhang, and Z. He, "Light Field Optimization for Optical Wireless Power Transfer," IEEE Photonics J. **13**(1), 1–9 (2021).
10. D. H. Nguyen, T. Matsushima, C. Qin, and C. Adachi, "Toward Thing-to-Thing Optical Wireless Power Transfer: Metal Halide Perovskite Transceiver as an Enabler," Front. Energy Res. **9**, 679125 (2021).
11. W. Fang, H. Deng, Q. W. Liu, M. Q. Liu, Q. W. Jiang, L. Q. Yang, and G. B. Giannakis, "Safety Analysis of Long-Range and High-Power Wireless Power Transfer Using Resonant Beam," IEEE Trans. Signal Process. **69**, 2833–2843 (2021).
12. N. B. Chichkov, A. Yadav, A. V. Kovalev, S. V. Smirnov, M. Herper, K. A. Fedorova, E. A. Viktorov, and E. U. Rafailov, "Pulse dynamics in SESAM-free electrically pumped VECSEL," Opt. Express **28**(9), 13466–13481 (2020).
13. T. Malica, J. P. Lin, T. Ackemann, D. J. Little, J. P. Toomey, D. Paboeuf, W. Lubeigt, N. Hempler, G. Malcolm, G. T. Maker, and D. M. Kane, "Mapping the dynamical regimes of a SESAM mode-locked VECSEL with a long cavity using time series analysis," Opt. Express **26**(13), 16624–16638 (2018).
14. J. Fakidis, H. Helmers, and H. Haas, "Simultaneous Wireless Data and Power Transfer for a 1-Gb/s GaAs VCSEL and Photovoltaic Link," IEEE Photonics Technol. Lett. **32**(19), 1277–1280 (2020).
15. W. W. Chow and S. W. Koch, *Semiconductor-laser fundamentals: physics of the gain materials* (Springer Science & Business Media, 1999).
16. X. S. Liu and W. Zhao, "Technology Trend and Challenges in High Power Semiconductor Laser Packaging," in IEEE 59th Electronic Components and Technology Conference (San Diego, CA, 2009), pp. 2106–2113.
17. B. Rösener, N. Schulz, M. Rattunde, C. Manz, K. Köhler, and J. Wagner, "GaSb-based VECSEL exhibiting multiple-watt output power and high beam quality at a lasing wavelength of 2.25 µm," Proc. SPIE **6997**, 699702 (2008).
18. J. E. Hastie, S. Calvez, M. D. Dawson, T. Leinonen, A. Laakso, J. Lyytikainen, and M. Pessa, "High power CW red VECSEL with linearly polarized TEM_{00} output beam," Opt. Express **13**(1), 77–81 (2005).
19. J. E. Hastie, L. G. Morton, A. J. Kemp, M. D. Dawson, A. B. Krysa, and J. S. Roberts, "Tunable ultraviolet output from an intracavity frequency-doubled red vertical-external-cavity surface-emitting laser," Appl. Phys. Lett. **89**(6), 061114 (2006).
20. M. Wichmann, M. K. Shakfa, F. Zhang, B. Heinen, M. Scheller, A. Rahimi-Iman, W. Stolz, J. V. Moloney, S. W. Koch, and M. Koch, "Evolution of multi-mode operation in vertical-external-cavity surface-emitting lasers," Opt. Express **21**(26), 31940–31950 (2013).
21. K. Nechay, A. Mereuta, C. Paranthoen, G. Brevalle, C. Levallois, M. Alouini, N. Chevalier, M. Perrin, G. Suruceanu, A. Caliman, E. Kapon, and M. Guina, "High-Power 760 nm VECSEL Based on Quantum Dot Gain Mirror," IEEE J. Quantum Electron. **56**(4), 1–4 (2020).
22. S. Ranta, M. Tavast, T. Leinonen, R. Epstein, and M. Guina, "Narrow linewidth 1118/559 nm VECSEL based on strain compensated GaInAs/GaAs quantum-wells for laser cooling of Mg-ions," Opt. Mater. Express **2**(8), 1011–1019 (2012).
23. M. Gaulke, J. Heidrich, BÖ Alaydin, M. Golling, A. Barh, and U. Keller, "High average output power from a backside-cooled 2-µm InGaSb VECSEL with full gain characterization," Opt. Express **29**(24), 40360–40373 (2021).
24. T. Schwarzbäck, H. Kahle, M. Eichfelder, W. M. Schulz, and P. Michler, "Generation of UV laser light via intra-cavity frequency doubling of an AlGaInP-VECSEL," in CLEO/Europe and EQEC 2011 Conference Digest, OSA Technical Digest (CD) (Optica Publishing Group, 2011), paper CB6_2.
25. E. Kantola, T. Leinonen, S. Ranta, M. Tavast, J.-P. Penttinen, and M. Guina, "1180 nm VECSEL with 50 W output power," Proc. SPIE 9349, 93490U (2015).
26. M. Kuznetsov, *VECSEL Semiconductor Lasers: A Path to High-Power, Quality Beam and UV to IR Wavelength by Design* (Wiley Online Library, 2010).
27. J. V. Moloney, I. Kilen, A. Bäumner, M. Scheller, and S. W. Koch, "Nonequilibrium and thermal effects in mode-locked VECSELs," Opt. Express **22**(6), 6422–6427 (2014).
28. M. Guina, A. Rantamäki, and A. Härkönen, "Optically pumped VECSELs: review of technology and progress," J. Phys. D: Appl. Phys. **50**(38), 383001 (2017).
29. A. C. Tropper and S. Hoogland, "Extended cavity surface-emitting semiconductor lasers," Prog. Quantum Electron. **30**(1), 1–43 (2006).
30. E. Kantola, T. Leinonen, S. Ranta, M. Tavast, and M. Guina, "High-efficiency tunable yellow-orange VECSEL with an output power of 20 W," Proc. SPIE **8966**, 89660D (2014).
31. B. Rudin, A. Rutz, M. Hoffmann, D. J. H. C. Maas, A.-R. Bellancourt, E. Gini, T. Südmeyer, and U. Keller, "Highly efficient optically pumped vertical-emitting semiconductor laser with more than 20 W average output power in a fundamental transverse mode," Opt. Lett. **33**(22), 2719–2721 (2008).

Optics EXPRESS

32. S. Binghua, X. Junwen, S. Lu, Z. Huiyuan, and P. Xuedan, "Generalised ABCD matrix treatment for laser resonators and beam propagation," Opt. Laser Technol. **43**(7), 1318–1320 (2011).
33. H. Kogelnik and T. Li, "Laser Beams and Resonators," Appl. Opt. **5**(10), 1550–1567 (1966).
34. B. Tromborg, J. Osmundsen, and H. Olesen, "Stability analysis for a semiconductor laser in an external cavity," IEEE J. Quantum Electron. **20**(9), 1023–1032 (1984).
35. M. Kuznetsov, F. Hakimi, R. Sprague, and A. Mooradian, "High-power (> 0.5-W CW) diode-pumped vertical-external-cavity surface-emitting semiconductor lasers with circular TEM_{00} beams," IEEE Photonics Technol. Lett. **9**(8), 1063–1065 (1997).
36. J.-P. Tourrenc, S. Bouchoule, A. Khadour, J.-C. Harmand, A. Miard, J. Decobert, N. Lagay, X. Lafosse, I. Sagnes, and L. Leroy, "Thermal optimization of 1.55 μm OP-VECSEL with hybrid metal–metamorphic mirror for single-mode high power operation," Opt. Quantum Electron. **40**(2-4), 155–165 (2008).
37. T. Lin, R. Sun, H. Sun, E. Guo, Y. Duan, N. Lin, X. Ma, and Y. Wang, "Material research on the InGaAs-emitting-layer VECSEL grown on GaAs substrate," Mater. Sci. Semicond. Process. **42**(3), 283–287 (2016).
38. C. H. McMahon, J. W. Bae, C. S. Menoni, D. Patel, H. Temkin, P. Brusenbach, and R. Leibenguth, "Detuning of the gain and reflectivity spectra and its effect on the output characteristics of vertical cavity surface emitting lasers," Appl. Phys. Lett. **66**(17), 2171–2173 (1995).